

Implementation and analysis of microcontroller based soft starters for three phase induction motors

Hamdy. A. Ashour and Rania. A. Ibrahim

Arab Academy for Science and Technology, Dept. of Electrical and Computer Control Eng., 1029 Miami, Alexandria, Egypt
hashour@aast.edu, rania_assem@alexseeds.com

This paper introduces two different microcontroller based three phase induction motor starters, the first using electromechanical star-delta with reactor starting and the second utilizes electronic AC voltage controllers starting technique. For each of the proposed methods, the experimental setup is implemented and the output voltage, current and speed waveforms were demonstrated and analyzed for different selection options and operating conditions. A dynamic model of three phase induction motor has been developed to validate a model of six terminals connection motor for star and delta performance analysis. The model has been utilized for the simulation analysis and comparison of various electromechanical and electronic induction motor starters techniques. Comparison between commercial analog controller based soft starter LH4-N2 and the proposed starter has been introduced as well. Experimental and simulation waveforms obtained are matched validating the proposed starters for practical applications.

هذا البحث يقدم نوعين من بادئات الحركة لمحركات الحث الثلاثي الأوجه التي تعتمد علي إستخدام المتحكم المتناهي الصغر (Microcontroller). الطريقة الأولى، وهي طريقة إلكتروميكانيكية، تعتمد علي توصيل محركات الحث الثلاثي star-delta مع إستخدام ملف. أما الطريقة الثانية فهي طريقة إلكترونية تعتمد علي إستخدام مغيرات الجهد المتردد وإلكترونيات القوي للحصول علي بادئات الحركة الناعمة. تم تنفيذ كل طريقة من الطرق المطروحة مع أخذ نتائج عملية للجهد و التيار والسرعة عند نقاط تشغيل مختلفة. أيضاً، تم عمل نموذج رياضي لمحركات الحث الثلاثي الأوجه بإستخدام المعادلات الديناميكية لحركة تلك المواتير وتم محاكاة النظام بإستخدام Matlab-Simulink كما تم إختبار هذا النموذج علي وسائل بدء الحركة المختلفة سواء كانت إلكتروميكانيكية أو إلكترونية مع دراسة كل وسيلة من هذه الوسائل. تم عمل مقارنة معملية بين بادئ الحركة الإلكتروني الذي تم تصميمه وتنفيذه مع بادئ الحركة الإلكتروني وهو أحد بادئات الحركة التي توفرها شركة Schneider في الأسواق. تم مطابقة النتائج النظرية والمعملية مما يؤيد إمكانية إستخدام أنواع بادئات الحركة المقترحة في التطبيقات العملية المختلفة.

Keywords: Dynamic modeling, Microcontrollers, Power electronics, Soft starters, Three phase induction motor

1. Introduction

Three phase induction motors are considered the universal work horses of industry, converting up to 80% of all electrical power into mechanical energy and cover up many heavy industrial applications such as fans, blowers, compressors, mixers, conveyors ...etc. Controlling the starting performance of three phase induction motors have always been the interest of many researchers, to develop varies techniques in order to control the starting transients associated with induction motors [1-12]. The need for reduced starting current condition not only reduces the stresses on the power utility, but also decreases the stresses on the motor and driven equipment, reduces overload and under

voltage relay trips and increases the number of start/stop times of the motor itself per day [1]. Many methods have been introduced for starting induction motors. Basically, they can be divided into two major groups; electromechanical starters and electronic starters [2]. The name electromechanical starters stems from the fact that they employ electromechanical contactors, relays, resistances and transformers for offering reduced voltage starting. Under this type of starters, methods such as Direct Online starting (DOL), star-delta starting, stator resistance starting and autotransformer starting are listed. As for the electronic starters, there are the AC voltage controller starters and V/F starters. Choosing the type of motor starter for each application depends on the motor characteristics,

available space, load torque requirements and overall cost. This paper introduces two microcontroller based soft starting techniques, the first is an electromechanical type using PIC16F84 in starting three phase induction motors in star-delta with series inductor starter, and the second is an electronic type using PIC16F877 as AC voltage controller starter. Both methods have been examined and experimental setups have been implemented for practical validation.

2. Induction motor modeling

Induction motor modeling has been discussed in many literatures [3-5]. Through the paper and for simulation purposes, induction motor modeling has been carried out using Simulink under Matlab in order to predict motor performance for each starting technique. To facilitate the connection of the three phase induction motor in star or delta configuration, the three phase supply voltage fed to the motor has been transformed to corresponding current sources. The block diagram representing the three phase induction motor dynamic model and the flow of variables is shown in fig. 1, while the corresponding equations based on the usage of stationary frame can be summarized as follows [6].

$$\begin{bmatrix} V_{d_s} \\ V_{q_s} \\ V_0 \end{bmatrix} = \sqrt{\frac{2}{3}} \begin{bmatrix} \cos(0) & \cos\left(\frac{2\pi}{3}\right) & \cos\left(\frac{4\pi}{3}\right) \\ \sin(0) & \sin\left(\frac{2\pi}{3}\right) & \sin\left(\frac{4\pi}{3}\right) \\ \frac{1}{\sqrt{2}} & \frac{1}{\sqrt{2}} & \frac{1}{\sqrt{2}} \end{bmatrix} \begin{bmatrix} V_{a_s} \\ V_{b_s} \\ V_{c_s} \end{bmatrix} \quad (1)$$

And for squirrel cage induction motor $\begin{bmatrix} V_{d_r} \\ V_{q_r} \end{bmatrix} = \begin{bmatrix} 0 \\ 0 \end{bmatrix}$

$$I = \int -L^{-1}RI + \int L^{-1}(V - G\omega_r I) \quad (2)$$

Where

$$I = \begin{bmatrix} I_{d_s} \\ I_{q_s} \\ I_{d_r} \\ I_{q_r} \end{bmatrix}, V = \begin{bmatrix} V_{d_s} \\ V_{q_s} \\ V_{d_r} \\ V_{q_r} \end{bmatrix}, R = \begin{bmatrix} R_s & 0 & 0 & 0 \\ 0 & R_s & 0 & 0 \\ 0 & 0 & R_r & 0 \\ 0 & 0 & 0 & R_r \end{bmatrix}$$

$$L = \begin{bmatrix} L_s & 0 & M & 0 \\ 0 & L_s & 0 & M \\ M & 0 & L_r & 0 \\ 0 & M & 0 & L_r \end{bmatrix}, G = \begin{bmatrix} 0 & 0 & 0 & 0 \\ 0 & 0 & 0 & 0 \\ 0 & M & 0 & L_r \\ -M & 0 & -L_r & 0 \end{bmatrix}$$

$$I_0 = V_0 \left[\frac{1}{(R_s + l_s s)} \right] \quad (3)$$

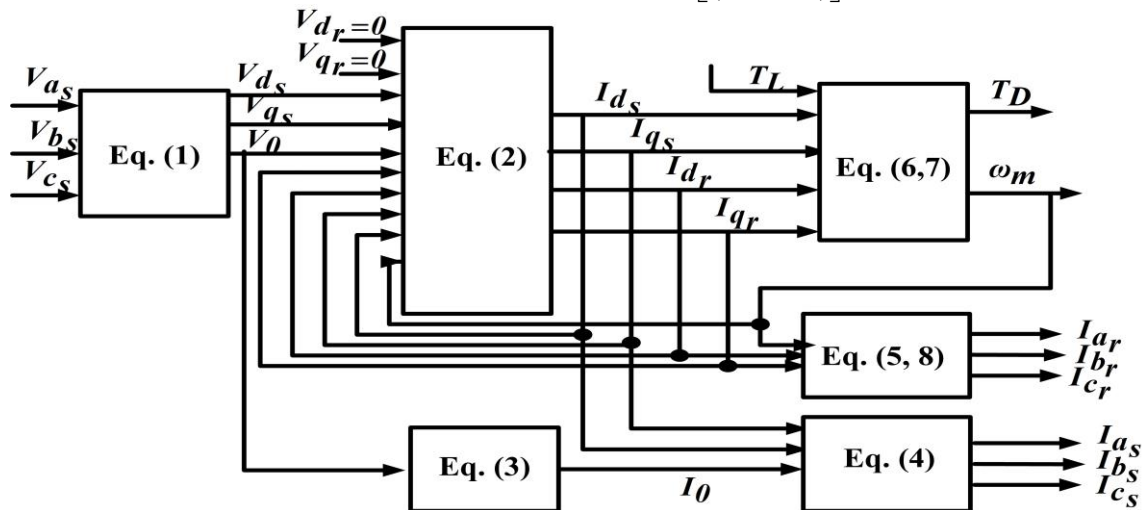


Fig. 1. Flow of variables and equations used in modeling of three phase induction motor in stationary reference frame.

$$\begin{bmatrix} I_{a_s} \\ I_{b_s} \\ I_{c_s} \end{bmatrix} = \sqrt{\frac{2}{3}} \begin{bmatrix} \cos(0) & \sin(0) & \frac{1}{\sqrt{2}} \\ \cos\left(\frac{2\pi}{3}\right) & \sin\left(\frac{2\pi}{3}\right) & \frac{1}{\sqrt{2}} \\ \cos\left(\frac{4\pi}{3}\right) & \sin\left(\frac{4\pi}{3}\right) & \frac{1}{\sqrt{2}} \end{bmatrix} \begin{bmatrix} I_{d_s} \\ I_{q_s} \\ I_0 \end{bmatrix} \quad (4)$$

$$\begin{bmatrix} I_{a_s} \\ I_{b_s} \\ I_{c_s} \end{bmatrix} = \sqrt{\frac{2}{3}} \begin{bmatrix} \cos(0) & \sin(0) \\ \cos\left(\frac{2\pi}{3}\right) & \sin\left(\frac{2\pi}{3}\right) \\ \cos\left(\frac{4\pi}{3}\right) & \sin\left(\frac{4\pi}{3}\right) \end{bmatrix} \begin{bmatrix} \cos \theta_r & \sin \theta_r \\ -\sin \theta_r & \cos \theta_r \end{bmatrix} \begin{bmatrix} I_{d_r} \\ I_{q_r} \end{bmatrix} \quad (5)$$

$$T_d = I^t G I. \quad (6)$$

$$\omega_m = \left(\frac{T_d - T_L}{(J_s + B)} \right). \quad (7)$$

$$\omega_r = \left(\frac{P}{2} \right) \omega_m, \quad \theta_r = \int \omega_r dt. \quad (8)$$

The overall model of the three phase induction motor has been simulated with Simulink under Matlab 6.5 and then grouped to form one block with 6 input stator terminals $a_1, b_1, c_1, a_2, b_2, c_2$, and T_L for load torque, while it outputs three phase stator and rotor currents $I_{s_{abc}}$ and $I_{r_{abc}}$, motor speed ω_r and motor developed torque T_d (see fig. 2). This dynamic model have been utilized to study and analyze different methods for the starting of three phase induction motor as will be described in the following sections.

3. Induction motor starting methods and dynamic analysis

If an induction motor is supplied from a fixed voltage at a constant frequency, the rotor current and developed torque can be determined as:

$$I_r = \frac{V_s}{\sqrt{\left(R_s + \frac{R_r}{S}\right)^2 + X_{eq}^2}}. \quad (9)$$

$$T_d = \frac{3R_r V_s^2}{S \omega_s [(R_s + \frac{R_r}{S})^2 + (X_{eq})^2]}. \quad (10)$$

Owing to the fact that at starting the slip is unity ($S=1$) and the motor is excited at full voltage, the induction motor absorbs a very high starting current and develops a high starting torque (that is proportional to the square of the supply voltage). Such high starting torque and current may cause damage to the mechanical equipment (such as hammering in fluid pumps) or voltage dips and unstable operation in working power supply sources (such as in stand alone diesel engine with synchronous generator on ships). In order to be able to reduce the starting current, starting voltage has to be controlled. Reduced voltage starters can be divided into: a) electromechanical soft starters, such as stator resistance, stator reactor, star-delta, and autotransformer starter, and b) electronic soft starters, such as AC voltage controller and V/F starters. In order to examine each method individually, simulation analysis has been carried out based on the dynamic model introduced in section (I) for each technique. Simulink block diagram of the star-delta starting as an example of simulated software techniques is shown in fig. 2, while the different simulated waveforms for different starting methods are depicted in figs. 3-a to fig. 3-g.

Comparison between DOL, stator resistance, stator reactor, star-delta, star-delta with inductor, autotransformer, AC voltage controllers using voltage ramp and using current limiting starting has been carried out for a three phase induction motor rated 0.75 hp, 380V, 1410 rpm motor. Based on simulation analysis of each technique, two sets of data are gathered, at no load and at 50% load, as to demonstrate the effect of loading on each of the starting techniques being tested. Rated DOL starting values at no load are taken as base values for the calculations of per unit starting voltage,

current and torque. The average energy losses calculated in table 1 are based on accumulated heat losses in both the stator and rotor over a definite time, which is chosen to be the same for all simulated starting techniques and after the motor starting period and reaching a steady state speed. As shown from table 1, the DOL method has the highest starting voltage, current and torque, while the soft starter with current limiter has the least values. As for the average energy losses, it is found that it is almost the same for all starting techniques, regardless of type of starter being used, except for resistance type starting because if the starting current increases, the acceleration time decreases and vice versa. The accumulated energy lost during a certain period of time will remain unchanged. The only technique which has high heat losses is the stator resistance start as it employs an additional resistance. It should be also noted that if the load is further increased more than 50% the load may be above the capability of the starter, thus producing very high energy losses that could damage the starter, the load and the motor as well. Choosing which one of these methods is most suitable, depends on the motor characteristics, starter features, application and the demands of each system. The differences between results in case of no-load and 50% load are very small since the motor rating is fractional horsepower. It should be noticed that values recorded in table 1 may be varied depending on motor parameters, load conditions, time of transition between different states and value of the applied supply voltage. In applications requiring speed control, advanced techniques such as V/F, vector and direct torque control of three phase induction motors are implemented. These techniques also provide an excellent starting performance for the motor but with extra high cost capacity to the previous starting methods particularly in higher power ratings.

4. Experimental implementation

Two methods for soft starting of three phase induction motors have been proposed based on microcontroller techniques, the first is an electromechanical type and is achieved

through the usage of star-delta with series inductor starting, while the second method is an electronic type and is done using TRIAC ac voltage controllers. Both methods have been implemented using PIC16F84 and PIC16F877 respectively, as simple and cost effective ways of digital control. Power circuits for both systems can be seen in fig. 4-a and fig. 5-a, while the PIC control circuits can be seen in fig. 4-b and fig. 5-b respectively.

4.1. Electromechanical star -delta with series reactor starter

Star -delta starting and reactor starting were introduced in [7], with each method operating individually and both were implemented using electromechanical contactors, relays and timers. Star-delta starting has limitations due to the fact that the starting applied voltage is reduced by $\sqrt{3}$ compared to the direct online method, which is a very narrow range. Also, the transition from star to delta causes voltage dips as the motor is momentarily disconnected from the supply (open transition). Combining star-delta starting with a reactor enhances the starting performance as will be seen through this work.

The proposed system uses a microcontroller to control the operation of the electromechanical contactors and relays. PIC16F84 provides a cheap and simple method for controlling the motor and contactors operation. External mechanical Timers are not needed when using the PIC16F84 since the delay times used are managed by the microcontroller itself, thus eliminating the cost of timers and reducing the overall cost. As seen from fig. 4, this type of starting consists of a three phase supply, three phase series inductor, main contactor (M), star contactor (Y), delta contactor (Δ), inductor contactor (L), PIC16F84 module, three phase circuit breaker and overload.

The PIC16F84 activates the M and Y contactor as soon as the start push button is pressed. After a delay time which can be set according to the operator through dip switches connected to the PIC16F84, the Y contactor is disconnected then the Δ contactor is activated. Finally, after another time delay, determined

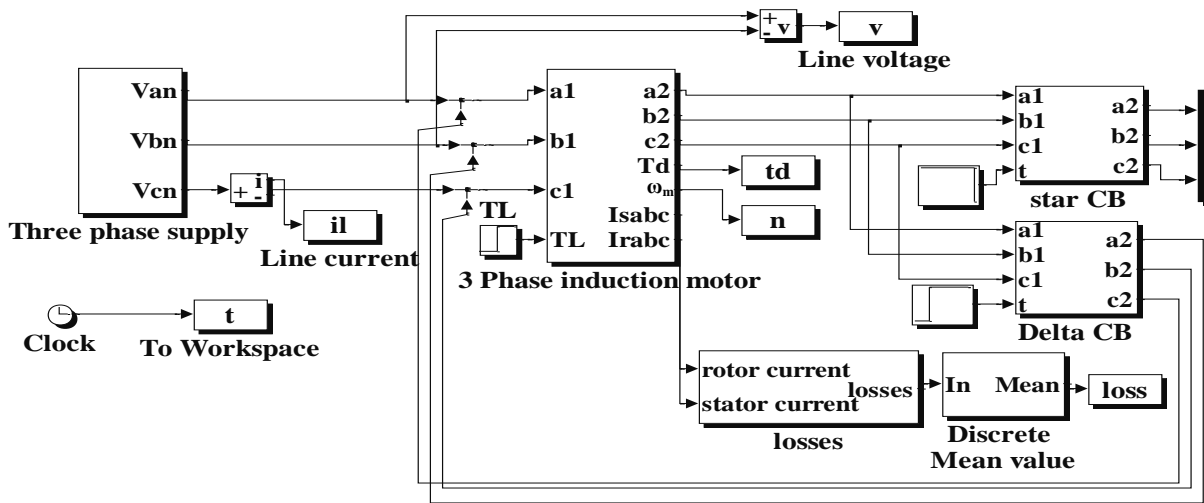
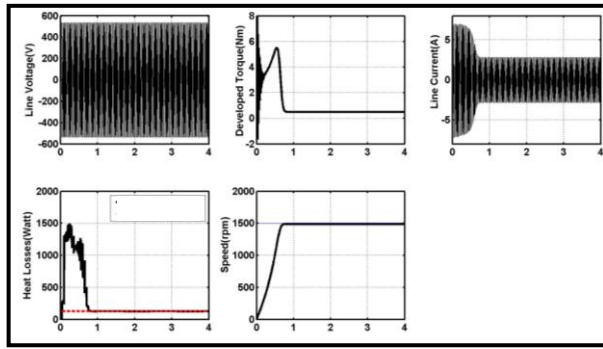


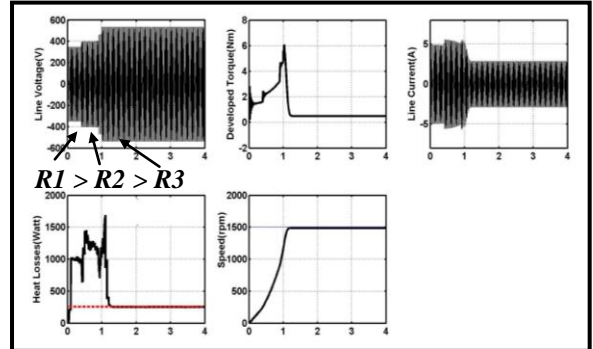
Fig. 2. Simulink diagram of star-delta as an example of the simulated starting methods.

Table 1
Comparison between different starting techniques

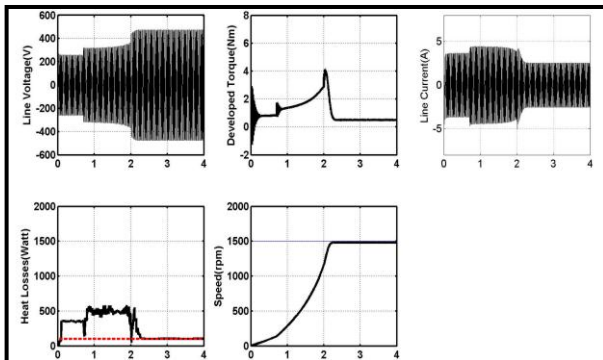
Method of starting	Starting voltage (p.u)		Starting current (p.u)		Starting load torque (p.u)		Acceleration time (sec)		Average energy losses (J)	
	No-load	50% load	No-load	50% load	No-load	50% load	No-load	50% load	No-load	50% load
	DOL	1	1	1	1.04	1	1.07	0.6	0.8	126.5
Sator resistance	0.65	0.65	0.7	0.72	0.3	0.34	1	1.2	249	254
Sator reactor	0.47	0.47	0.48	0.5	0.37	0.39	1.5	2.2	102	103.6
Star- delta	0.57	0.57	0.28	0.3	0.3	0.32	1.8	2.5	126	126.6
Star delta with inductor	0.45	0.45	0.4	0.43	0.2	0.21	2.4	3.3	126.4	126.7
Autotransformer	0.37	0.37	0.36	0.37	0.12	0.14	1.9	2.5	126.2	126.5
Soft starter (voltage ramp)	0.33	0.33	0.3	0.34	0.097	0.1	1.8	2.4	126	126.3
Soft starter (current limiter)	0.12	0.12	0.14	0.14	0.1	0.1	1.5	2.1	130	130.6



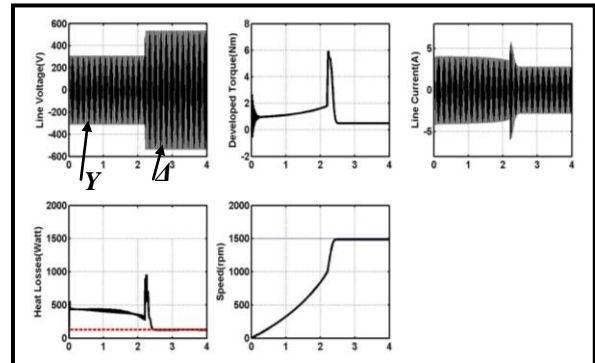
(a)



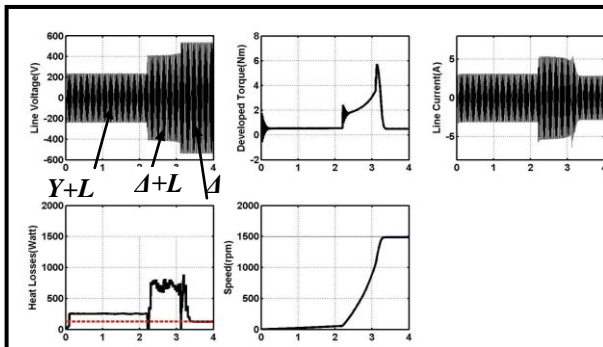
(b)



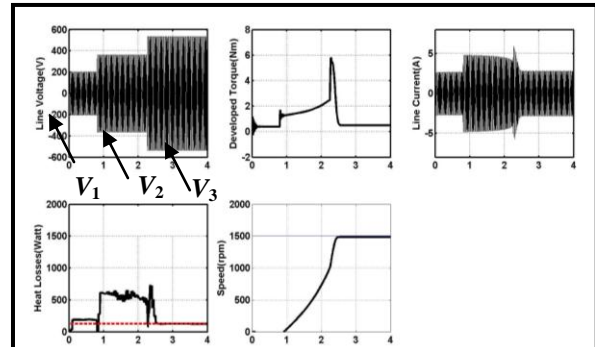
(c)



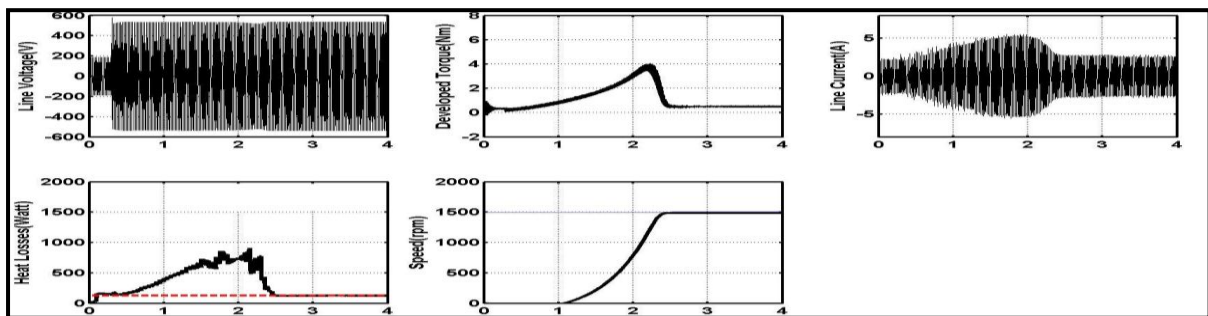
(d)



(e)



(f)



(g)

Fig. 3. Simulation waveforms of line voltage, developed torque, line current, $I^2 R$ losses and speed respectively (a) DOL (b) multi stepping stator resistance (c) multi stepping stator reactor (d) star-delta (e) star –delta through reactor (f) multi stepping auto- transformer (g) AC voltage controller.

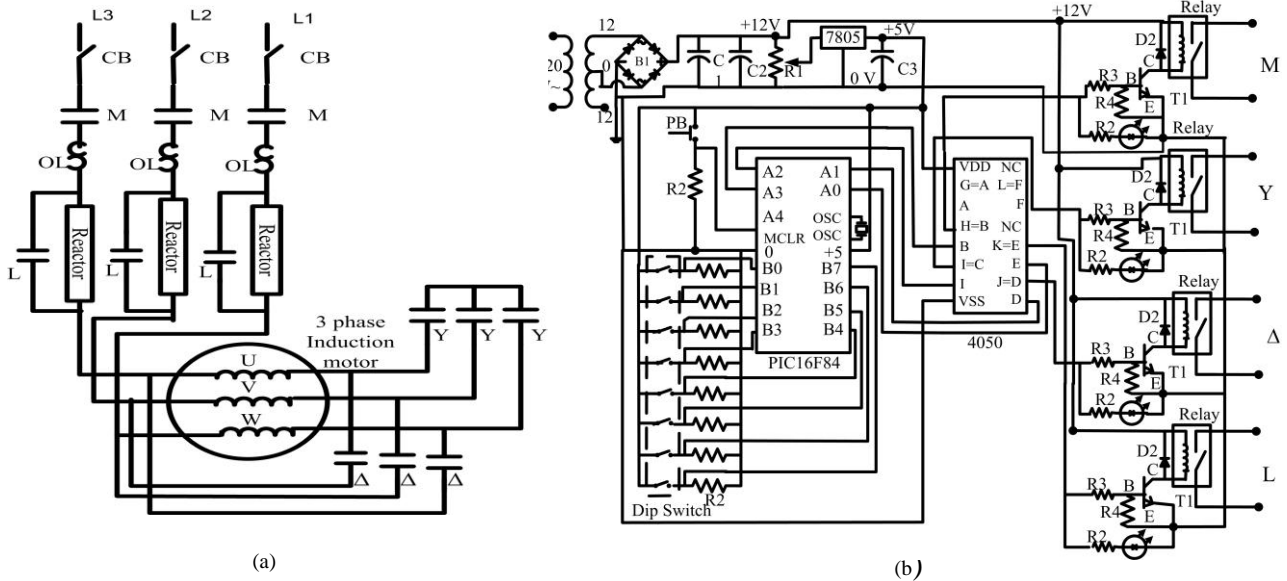


Fig. 4. First proposal: electromechanical star-delta with series inductor starting (a) power circuit (b) control circuit using PIC16F84.

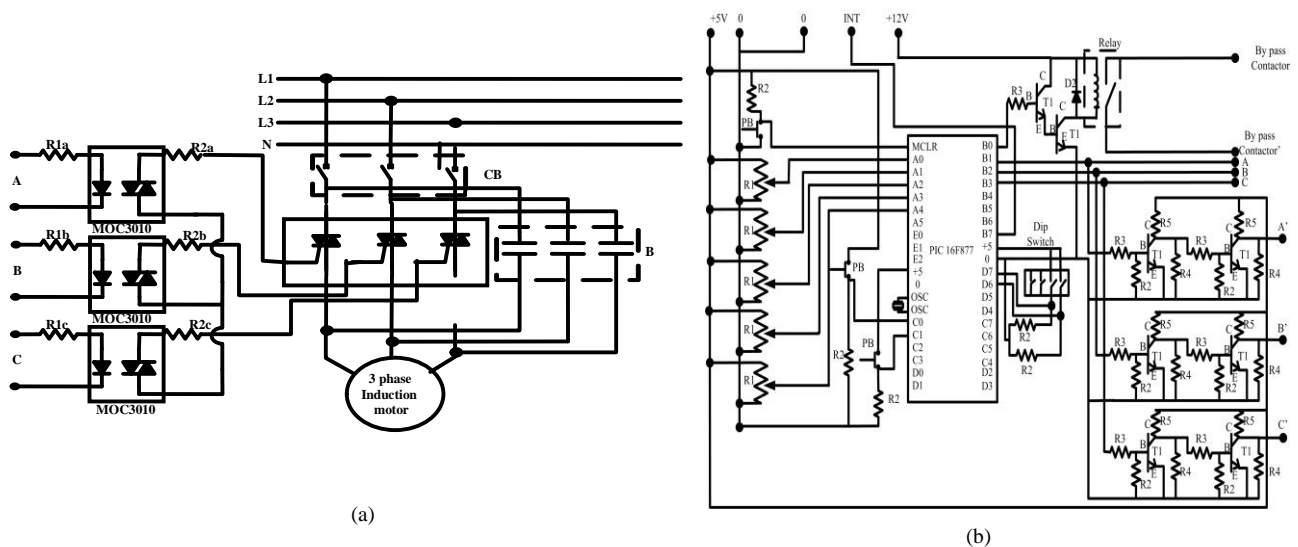


Fig. 5. Second proposal: electronic AC voltage controller starting (a) power circuit (b) control circuit using PIC16F877.

by the dip switches, the L contactor is activated, bypassing the series reactors. At any time if the main stop push button is pressed, the whole process terminates. The flow chart describing the program implemented in the PIC16F84 module in simple English like language (PDL) is depicted in fig. 6. The practical setup has been implemented as to be reliable and flexible such that it can be individually operated as a)

DOL b) DOL with M contactor only c) star-delta with M, Y and Δ contactors c) star-delta through inductors with M, Y, Δ and L contactors. The experimental setup has been tested on a squirrel cage induction motor of 1.5 kW, Δ / Y, 220 / 380 V, 6.75 / 3.9 A, 50 Hz, 1410 rpm. Different experimental waveforms for line voltage and current have been obtained as depicted in figs. 7- 11. As seen from fig. 7, the motor shows that using

direct online starting technique, the motor is started at full voltage, which corresponds to the maximum starting current that the motor can draw from the supply. The input line current to the motor at this case is equal to 10.6A, (3 times the rated current). In fig. 8, the motor is started with the star-delta technique; the motor stator windings are connected in using the Y contactor, where at this point the input voltage to the motor is 57% the rated voltage. The reduction in starting voltage causes reduction in starting current by 40% of the starting current, which is equal to only 1.2 times the rated current. After time delay, which is approximately 0.55 sec, the motor stator windings are Δ connected. Note that the Y contactor is disconnected first before the Δ operation in order not to cause any short circuit on the motor windings. The transition from Y to Δ causes a voltage spike that can be seen clearly. The voltage waveforms don't show any change since the displayed voltage is the supply line voltage applied to the motor and not the motor phase voltage. Starting in star delta with the addition of reactors can be seen

in fig. 9, at first, the motor is operated in Y connected stator windings with the series inductor and the M contactor on. At that time, the motor is started at nearly 50% of the rated voltage with starting current corresponding to 1.1 times the rated current only. After a time delay of 0.4 seconds, the motor is switched from Y to Δ with the M contactor and series inductors on. The transition from Y to Δ has been improved due to the series inductor and thus the voltage spike magnitude is reduced. At this point, the input voltage to the motor has been increased, corresponding to higher current. After another 0.3 seconds, the L contactor is switched on, bypassing the series inductor and allowing the motor to operate at full voltage with a Δ connected stator. Starting an induction motor with series inductors has a disadvantage of starting the motor at low power factor (lagging). In order to overcome this problem, shunt capacitors are added on motor windings, which improves the line power factor from lagging to approximately unity as can be seen from figs. 10 and 11.

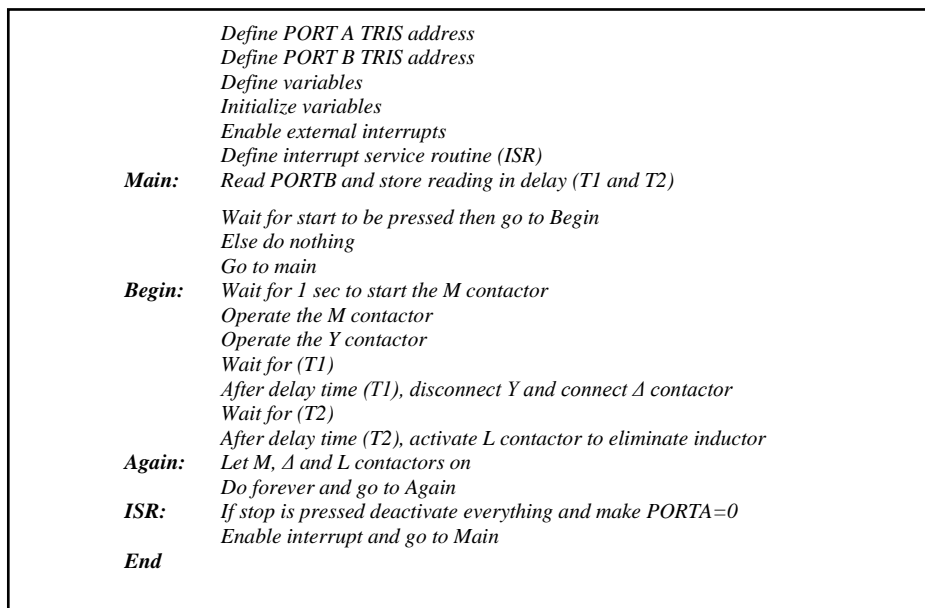


Fig. 6. PDL flow of implemented program of the star-delta with reactor starting.

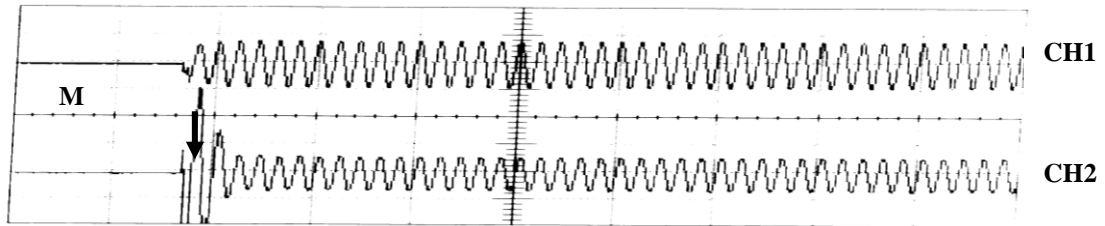


Fig. 7. DOL starting for squirrel cage motor, experimental supply line voltage and current waveforms. Scales: voltage 400 V/div, current: 6 A/div time, 0.1 sec/div.

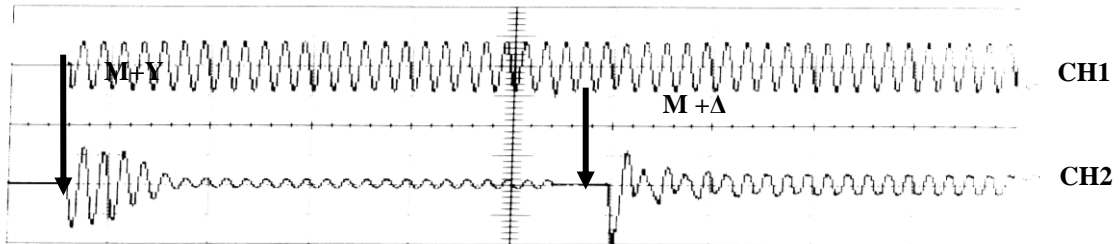


Fig. 8. Star-delta starting for squirrel cage motor, experimental supply line voltage and current waveforms. Scales: voltage 400 V/div, current: 6 A/div time, 0.1 sec/div.

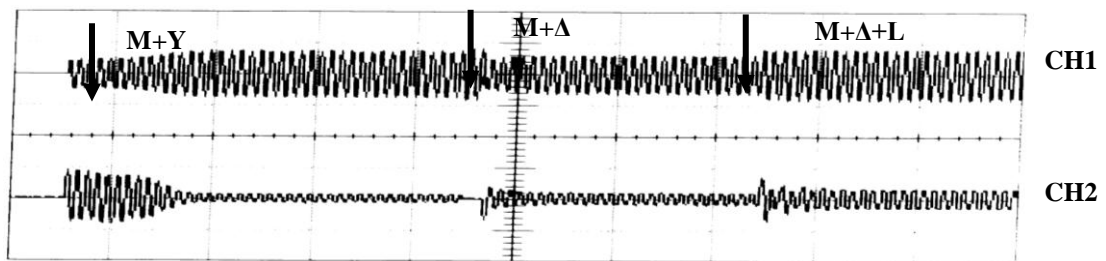


Fig. 9. Star-delta and inductor start for squirrel cage motor, experimental supply line voltage (after inductor) and line current waveforms. Scales, voltage 400 V/div, current, 6 A/div time, 0.2 sec/div.

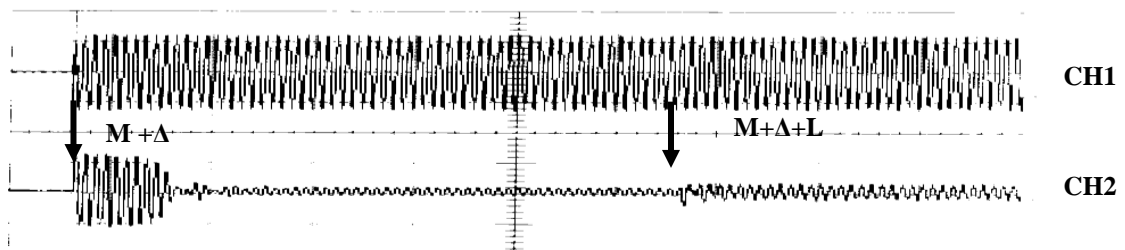


Fig. 10. Inductor start for squirrel cage motor with shunt capacitors, experimental supply line voltage (before inductor) and line current waveforms. Scales, voltage 400 V/div, current, 6 A/div time, 0.2sec/div.

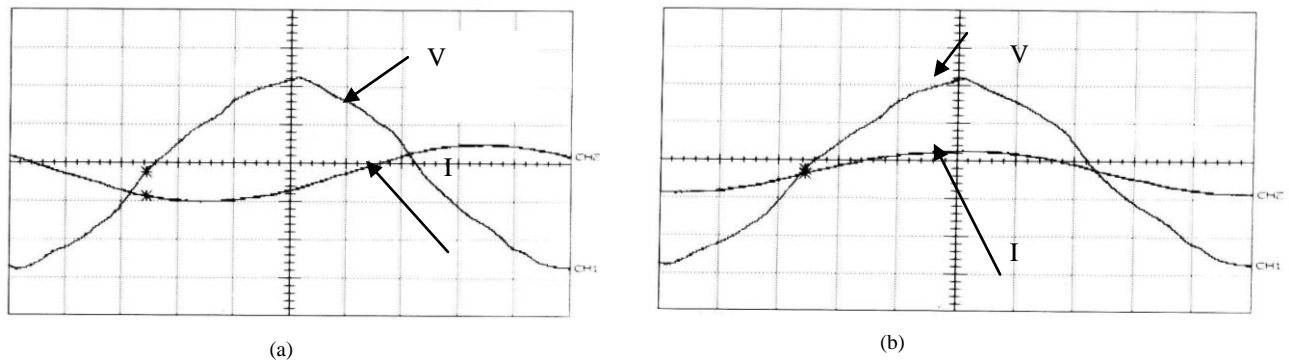


Fig. 11. Effect of adding shunt capacitors on power factor, experimental line voltage and line current waveforms (a) lagging power factor without capacitor (b) approximately unity power factor with capacitor. Scales, voltage 200 V/div, current, 3 A/div time, 2 msec/div.

Simulation analysis has been carried out based on the dynamic model introduced in section II in order to compare the theoretical results with the experimental waveforms. Figs. 13 and 14 show both simulation and experimental waveforms obtained from direct online starting and the proposed star-delta with series reactor starting technique respectively. From figs. 13 and 14 it can be seen that simulation and experimental waveforms are correlated well validating the setup for practical implementation in industrial applications.

4.2. Electronic AC voltage controller starter

AC motor starters employing power semiconductors are being increasingly used to replace the electromechanical starters because of their controlled soft-start capability with limited starting current [8-11]. As the name implies, this type of starters employs the usage of power electronic AC voltage controllers to vary the RMS voltage supplied to the motor using phase control technique, which is done by varying the delay angle α of the AC voltage controller being used. Comparison Analysis of different AC voltage controllers operation, control and configurations have been introduced by the authors in [12]. The main advantage of this type of starting is the smooth starting that can not be achieved by any other electromechanical starting procedure, which causes a very remarkable decrease in starting current. This type of soft starter has been

implemented by the authors using PIC16F877, which is more powerful than the PIC16F84 as it contains built-in A/D converter with multi channels. As seen from the general power circuit diagram in fig. 5-a, the DC power supply is used to offer any DC voltage needed to operate the PIC16F877 module, contactor (B) relay and the fans used for cooling the AC switches. The synchronization module is used to issue an interrupt signal at every zero crossing of the phase voltage of phase-a in order to allow the control of the delay angle α . The contactor B is being used to bypass the AC switch module after soft starting period has been accomplished, as to allow direct operation of the motor from the three phase supply and reduces the stresses on the TRIAC switches hence increases their life time. As for the PIC16F877, the microcontroller has been programmed to serve the following functions:

1. Motor soft starting: achieved by variation of α as measured from zero crossing of phase-a voltage, causing variation of supplied motor voltage resulting in smooth starting.
2. Selection of initial torque: This option is used to allow the motor at any desired starting voltage selected by the operator. This option facilitates the usage of soft starter in starting the motor with load, requiring high starting torque.
3. Selection of acceleration time (voltage ramp): This method controls the acceleration time of the motor, as to say, it controls the rate of change of α . This option provides the facility of starting smoothly high inertia loads and equipment such as belt conveyors.

4. By pass contactor feature: The PIC16F877 module allows the operation of contactor B to bypass the AC switches module after motor has reached rated speed and full voltage. This option allows the use of a single soft starter to start multi motors in sequence. Also, disconnecting the AC switches after full voltage achievement saves energy that is consumed due to switching of those devices and increases the total efficiency and life time.

5. Soft stop feature: This feature allows the smooth stopping of the motor and is achieved by incrementing a till achieving zero voltage condition. Soft stopping may be required for some particular applications such as water pumping systems.

6. Sudden stop capability: Selecting this feature, the motor is immediately disconnected from the supplying system. This method may be also used as an emergency stop for the motor.

The flow chart describing the program implemented in the PIC16F877 module in simple English like language (PDL) is shown in fig. 12. The electronic AC voltage controller starting experimental setup has been tested on an 3-ph squirrel cage induction motor2 of 0.3 kW, Δ / Y , 220 / 380 V, 1.2 / 0.7 A, 50 Hz, 1450 rpm. Different output waveforms for voltages, current and speed can be seen from fig. 15 to fig. 18 for different operating selection modes. Simulation analysis has been carried out for the proposed implemented soft starter using AC voltage controllers based on the model developed in section II. Figs. 19 and 20 depict the experimental and simulated waveforms for different operating conduction. The model has been implemented to be as flexible as the experimental setup in terms of the selection of starting torque and acceleration time ramp. Results shown in fig. 19 and fig. 20 illustrate the similarity of both the experimental and simulation waveforms for different operating conditions hence validating the experimental setup for real applications and the simulating model for more theoretical analysis and investigations for future works. Differences noticed between results arise from the fact that the model is linear and the response is sensitive to motor parameters and operating conditions. Experiments have been conducted on a

commercial analog controller based soft starter with model number LH4-N2 developed by SquareD Telemecanique whose rated at 3 kW. The LH4-N2 has the features of selecting initial torque (starting voltage), acceleration time (voltage ramp) and soft stop capability. Experimental comparison has been conducted between the LH4-N2 soft starter and the proposed implemented AC voltage controller soft starter on a three phase, Δ/Y 220/380 V, 1.2/ 0.7 A, 50 Hz, 300W, 1450 rpm induction motor. Experimental voltage and current wave forms obtained can be seen in fig. 21. The discontinuity of line current shown is arisen from the fact that commercial LH4-N2 soft starter is designed to start high inertia heavy loads and not light loads, such starter works better with a motor whose ratings are somewhere close to its ratings. This problem is overcome in the implemented soft starter where both the starting voltage and ramp time can be fully adjusted for light and heavy load conditions. Also the implemented AC voltage controller soft starter has the facility of bypass contactor, which is not valid in the commercial one, which is if needed, will add additional cost for the LH4-N2 soft starter. This feature is very useful to use one starter for multi motors starting in sequence and also reduces stresses and increases the life time of the starter. It should be noted that the cost of the implemented starter is almost half that of the commercial one.

5. Conclusions

Modeling and simulation of three phase induction motor has been implemented and tested for various starting techniques. The model has proven its validity and its flexibility in simulating different kinds of starting techniques. Two microcontroller based methods for soft starting of three phase induction motor were carried out, one using star-delta in combination with a reactor using PIC16F84 and the other using AC voltage controller starting using PIC16F877. Comparison with commercial soft starter LH4-N2 has been studied and the effectiveness with simplicity and low cost of both proposed starters have been demonstrated.

```

Define PORTA, PORTB, PORTC, PORTD TRIS address
Assign PORTA, PORTC, PORTD as input
Assign PORT B as output
Set PORTA, PORTB, PORTC, PORTD data address
Define interrupt service routine
Define variables
Set A/D conversion
Enable external interrupts (ISR)
Initialize A/D
Initialize variables
Repeat: If start is pressed go to Loop
Go to Repeat
Loop: Read dip switches for feature selections
Read A/D channels for starting voltage, start and stop voltage ramp
Scale and adjust limits for starting voltage and voltage ramps
Wait for interrupt
Go to Loop
Again: Do forever and wait for interrupt
Go to Again
ISR: If stop is pressed with sudden stop feature selected then
Deactivate bypass contactor
Disable interrupt and go to Repeat
End if
If stop is pressed and soft stop feature selected then
Deactivate bypass contactor
Begin soft stop feature by incrementing delay
Go check alpha mode at x
End if
If stop is not pressed then
Begin soft start by decrementing delay angle
Go check alpha mode at x
End if
x: If delay in mode 1 ( $120^\circ \leq \text{delay} \leq 180^\circ$ ) "almost zero voltage"
Output pulse to phase b
Output pulse to phase c after  $60^\circ$ 
Output pulse to phase a after another  $60^\circ$ 
End if
If delay angle in mode 2 ( $60^\circ \leq \text{delay} < 120^\circ$ )
Output pulse to phase c
Output pulse to phase a after  $60^\circ$ 
Output pulse to phase b after another  $60^\circ$ 
End if
If delay in mode 3 ( $\text{delay} < 60^\circ$ ) "full voltage"
Wait for a while
Send high signal to all three phases
Activate bypass contactor
End if
Enable interrupt and proceed program at Again
End
    
```

Fig. 12. PDL flow of implemented program of the AC voltage controller starting.

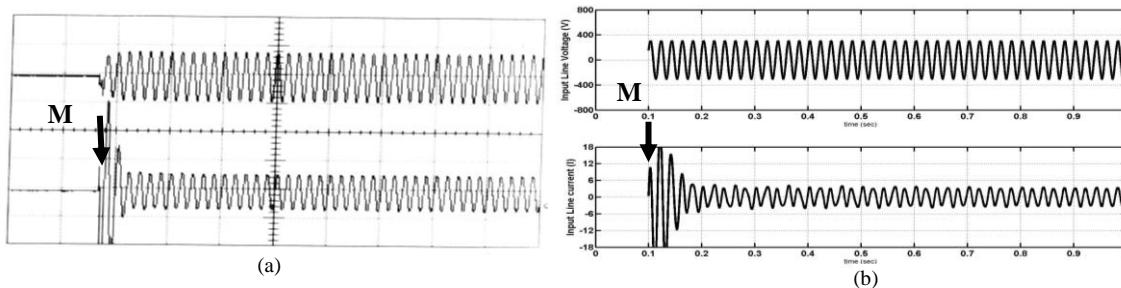


Fig. 13. DOL starting waveforms (a) experimental (b) simulation. Scales, Voltage 400 V/div, current, 6 A/div, time, 0.1 sec/div.

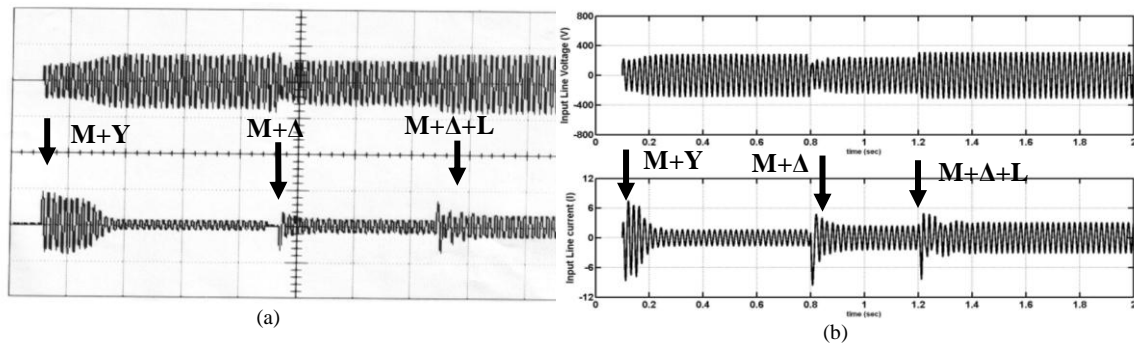


Fig. 14. Star -delta with reactor (inductor) start for inductance value of 30mH waveforms (a) experimental (b) simulation. Scales, Voltage 400 V/div, current, 6 A/div time, 0.2 sec/div.

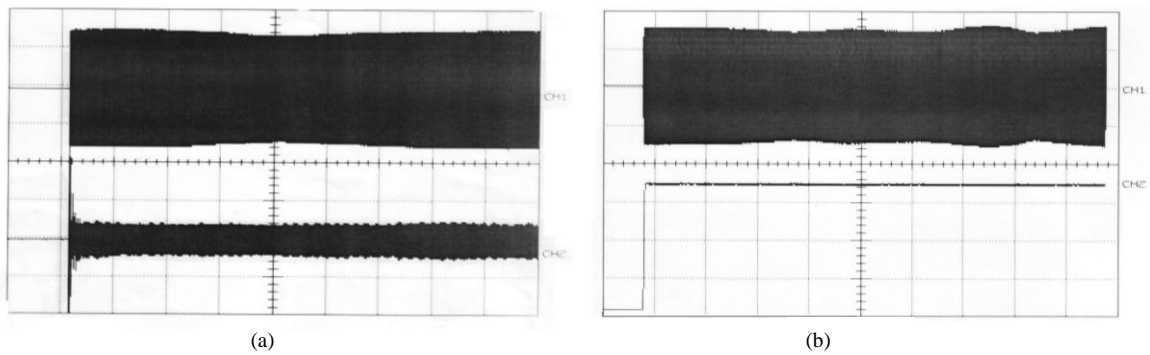


Fig. 15. DOL starting, experimental line voltage, line current and rotor speed waveforms (a) line voltage and line current (b) line voltage and speed. Scales, Voltage 400 V/div, current 1 A/div, speed, 400 rpm/div, time (a) 1 sec/div, time (b) 5 sec/div.

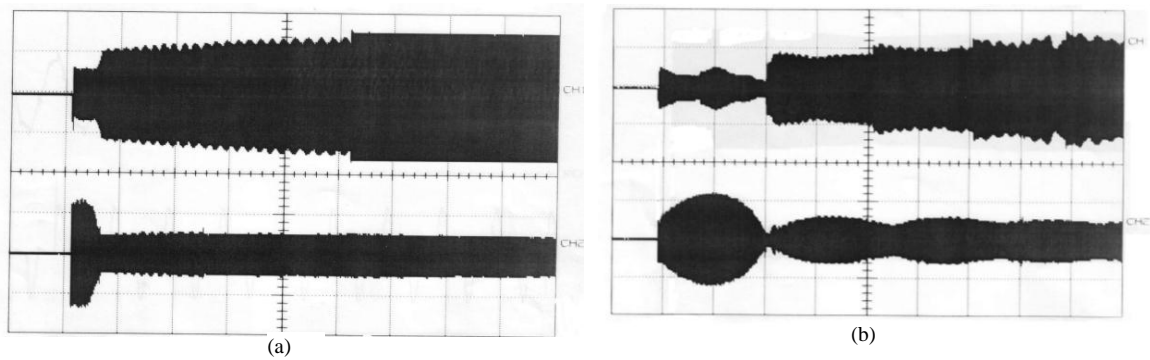


Fig. 16. AC voltage controller starting at different voltage ramps, experimental line voltage and line current waveforms (a) high voltage ramp (b) low voltage ramp. Scales, voltage 400 V/div, current 1 A/div, time, 1 sec/div.

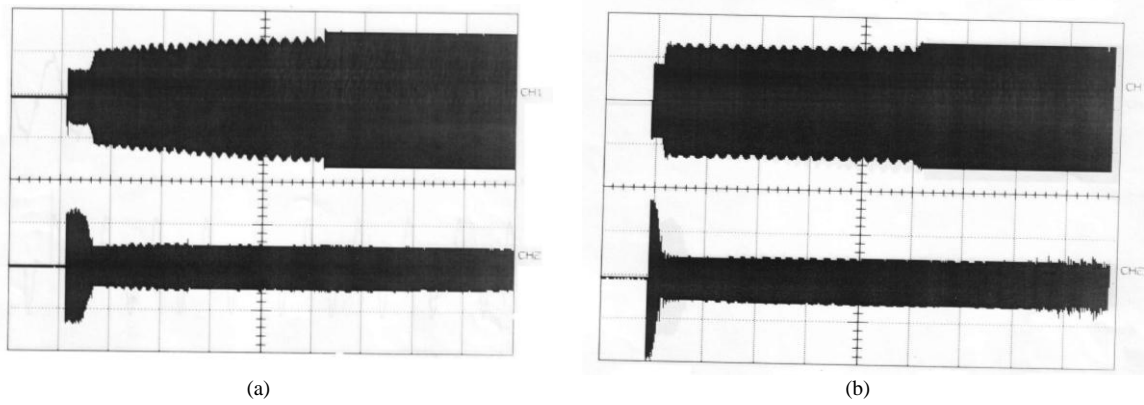


Fig. 17. AC voltage controller starting at different initial torques, experimental line voltage and current (a) low initial torque (b) high initial torque scales, voltage 400 V/div, current 1 A/div, time, 1 sec/div.

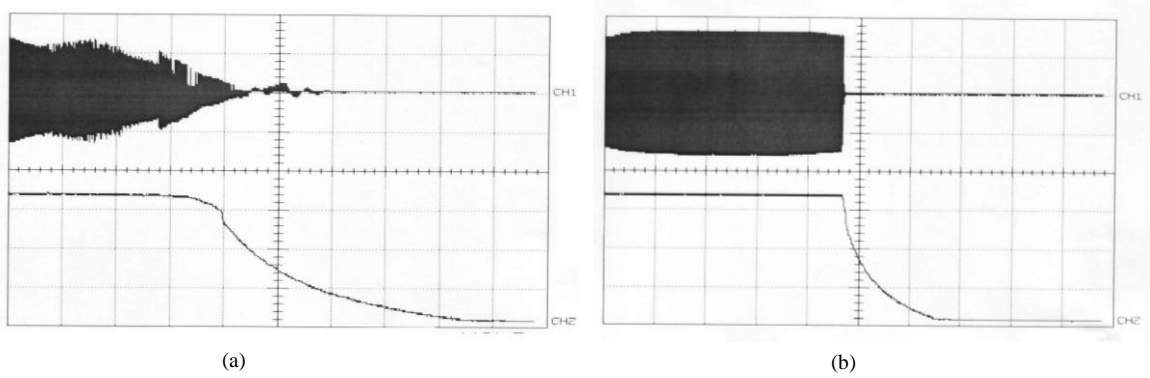


Fig. 18. Stopping of induction motor 2, experimental line voltage and speed waveforms (a) soft stop (b) sudden stop. Scales: Voltage 400 V/div, speed 400 rpm/div, time, 5 sec/div.

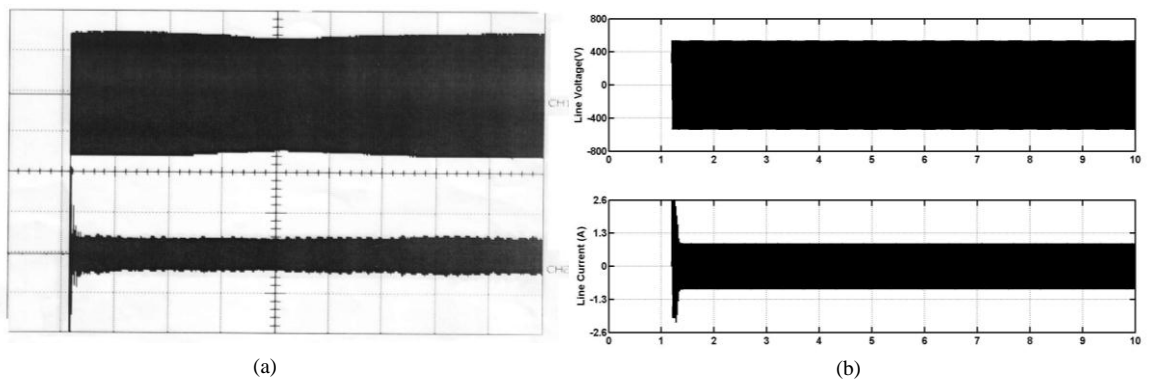


Fig. 19. Direct online starting waveforms (a) experimental (b) simulation. Scales, Voltage 400 V/div, current 1.3 A/div, time, 1 sec/div.

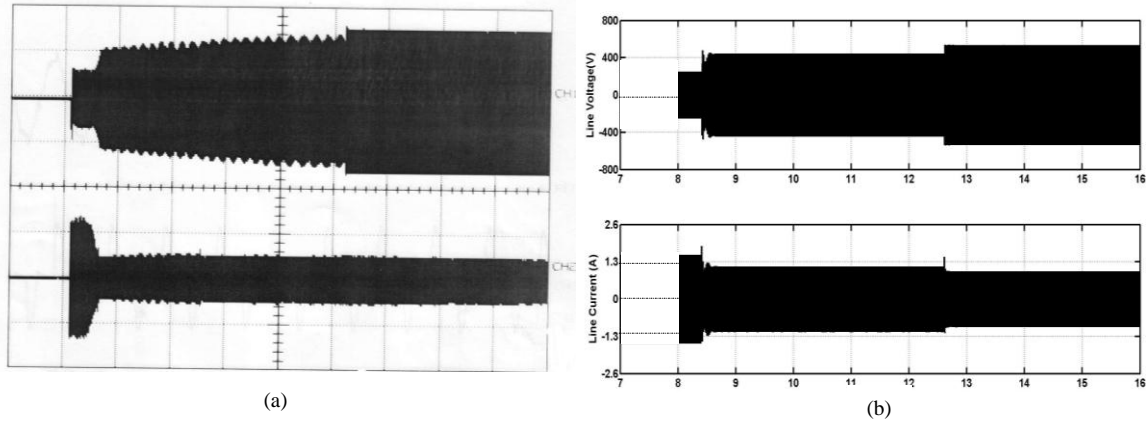


Fig. 20. Soft starting waveforms (a) experimental (b) simulation. Scales, voltage 400 V/div, current 1.3 A/div, time, 1 sec.

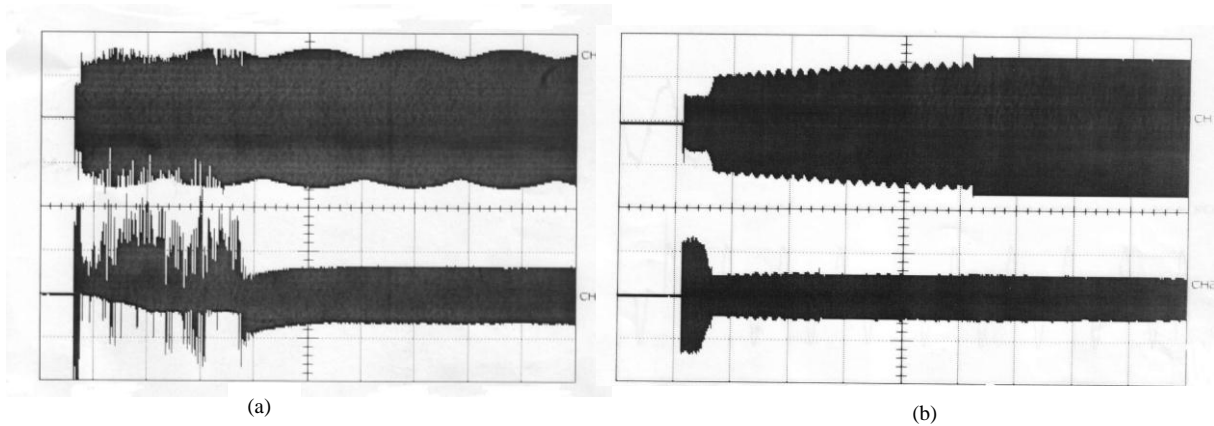


Fig. 21. Comparison between starting using the commercial LH4-N2 and implemented soft starter (a) the LH4-N2 (b) the implemented starter. Scales, voltage: 400 V/div, current: 1 A/div, time, 1 sec/div.

List of symbols

V_{d_s}, V_{q_s} are the direct and quadrature axis stator voltages,
 V_0, I_0 are the zero sequence stator voltage and current,
 $V_{a_s}, V_{b_s}, V_{c_s}$ are the phase a, b and c stator voltages,
 $I_{a_s}, I_{b_s}, I_{c_s}$ are the phase a, b and c stator currents,
 $I_{a_r}, I_{b_r}, I_{c_r}$ are the phase a, b and c rotor currents,
 I_{d_r}, I_{q_r} are the direct and quadrature axis rotor currents,
 I_{d_s}, I_{q_s} are the direct and quadrature axis stator currents,
 M is the mutual inductance,

P is the number of stator poles,
 θ_r is the rotor angle in radians,
 ω_m, ω_r are the mechanical and electric angular velocity in rad/sec,
 R_s, L_s, l_s are the stator resistance, self and leakage inductance,
 R_r, L_r are the rotor resistance and self inductance referred to stator,
 X_{eq} are the equivalent reactance = $(X_s + X_r)$,
 X_s, X_r are the stator and rotor inductive reactances,
 J is the moment of inertia,
 B is the friction co-efficient,
 T_d, T_L are the developed motor and load torque,
 α is the delay angle,
 s is the laplace operator, and
 S is the slip.

References

- [1] J.A. Kay, R.H. Paes, G. Seggewiss and R.G. Ellis, "Methods for the Control of Large Medium-Voltage Motors: Application Considerations and Guidelines", IEEE Trans. Industry Applications, Vol. 36 (6), pp. 1688-1696, November/ December (2000).
- [2] R.F. McElveen and M.K. Toney, "Starting High-Inertia Loads", IEEE Trans. Industry Applications, Vol. 37 (1), pp. 137-144, January/ February (2001).
- [3] M.G. Solveson, B. Mirafzal and N.A.O. Demerdash, "Soft-Started Induction Motor Modeling and Heating Issues for Different Starting Profiles Using a Flux Linkage ABC Frame of Reference", IEEE Trans. Industry Applications, Vol. 42 (4), pp. 973-982, July/ August (2001).
- [4] G. Zenginobuz, I. Çadircı, M. Ermiş and C. Barlak, "Soft Starting of Large Induction Motors at Constant Current With Minimized Starting Torque Pulsations", IEEE Trans. Industry Applications, Vol. 37 (5), pp. 1334-1347, September/ October (2002).
- [5] G. Zenginobuz, I. Çadircı, M. Ermiş and C. Barlak, "Performance Optimization of Induction Motors During Voltage-Controlled Soft Starting", IEEE Trans. Energy Conversion, Vol. 19 (2), pp. 278-288, June (2004).
- [6] A.K. Mukhopadhyay, "Matrix Analysis of Electrical Machines", New Age International Limited Publishers, Ch. 7, pp. 77- 104 (2003).
- [7] J. Nevelsteen and H. Aragon, "Starting of Large Motors-Methods and Economics", IEEE Trans. Industry Applications, Vol. 25 (6), pp. 1012-1018, November/ December (1989).
- [8] V.V. Sastry, M.R. Prasad and T.V. Sivakumar, "Optimal Soft Starting of Voltage- Controller Fed IM Drive Based on Voltage Across Thyristor", IEEE Trans. Power Electronics, Vol. 12 (6), pp. 1041-1051, November (1997).
- [9] I. Çadircı, M.Ermiş, E. Nalçacı, B.Ertan and M. Rahman, "A Solid State Direct On Line Starter for Medium Voltage Induction Motors with Minimized Current and Torque Pulsations", IEEE Trans. Energy Conversion, Vol. 414 (3), pp. 402- 412, September (1999).
- [10] A. Ginart, R. Esteller, A. Maduro, R. Pifero and R. Moncada, "High Starting Torque for AC SCR Controller", IEEE Trans. Energy Conversion, Vol. 14 (3), pp. 553-559, September (1999).
- [11] A. Gastli and M.M. Ahmed, "ANN-Based Soft Starting of Voltage-Controlled- Fed IM Drive System", IEEE Trans. Energy Conversion, pp. 1- 7 (2005).
- [12] H.A. Ashour and R.A. Ibrahim, "Comparison Analysis of AC Voltage Controllers Based on Experimental and Simulated Application Studies", ICCES Cairo-Egypt, Ain Shams University, pp. 79-84, November (2006).

Received April 14 12, 2007

Accepted September 9, 2007